5

PID control with gravity compensation for hydraulic 6-DOF parallel manipulator

Chifu Yang*, Junwei Han
O.Ogbobe Peter, and Qitao Huang
State Key Laboratory of Robotics and System,, Harbin Institute of Technology, Harbin, Heilongjiang, 150001, China

Abstract

A novel model-based controller for 6 degree-of-freedom (DOF) hydraulic driven parallel manipulator considering the nonlinear characteristic of hydraulic systems-proportional plus derivative with dynamic gravity compensation controller is presented, in order to improve control performance and eliminate steady state errors. In this paper, 6-DOF parallel manipulator is described as multi-rigid-body systems, the dynamic models including mechanical system and hydraulic driven system are built using Kane method and hydromechanics methodology, the numerical forward kinematics and inverse kinematics is solved with Newton-Raphson method and close-form solutions. The model-based controller is developed with feedback of actuator length, desired trajectories and system states acquired by forward kinematics solution as the input and servovalve current as its output. The hydraulic system is decoupled by local velocity compensation in inner control loop prerequisite for the controller. The performance revolving stability, accuracy and robustness of the proposed control scheme for 6-DOF parallel manipulator is analyzed in theory and simulation. The theoretical analysis and simulation results indicate the controller can improve the control performance and eliminate the steady state errors of 6-DOF hydraulic driven parallel manipulator.
Keywords: Parallel manipulator; Proportional-derivative control; Hydraulic servo-systems; Dynamic compensation

*Correspondence to: C.F Yang, State Key Laboratory of Robotics and System, Harbin Institute of Technology, Harbin, Heilongjiang, 150001, China.
E-mail: ycf1008@163.com; Tel: +86-451-86412548(325); Fax: +86-451-86412258

Contract/grant sponsor: China Academy of Space Technology;
contract/grant number: HgdJG00401D04
Contract/grant sponsor: State Key Laboratory of Robotics and System (HIT);
contract/grant number: SKLRS200803B

1. Introduction

Hydraulic driven 6-DOF parallel manipulator with long stroke actuators and heavy load is applied in most of the current high fidelity simulators, which is used to simulate various motions in different environments by exporting varying position and orientation. There are several advantages in the application of hydraulic driven parallel manipulator which includes large output force and torque, higher rigidity and accuracy due to the parallel path and averaged link to end effectors error, compared with serial manipulator [1-2]. A classical proportional plus integral plus derivative controller is applied in hydraulic driven 6-DOF parallel manipulator continually due to easy to implementation [3], nevertheless the existence of large steady state errors and dynamic errors in virtue of the influence of system gravity taken no account of hydraulic and mechanical systems in classical proportional plus integral plus derivative control system may degrade the control performance. Well-known facts, it is very difficult for the classical PID control to satisfy the requirements, less steady state error and superior dynamic performance simultaneously. With respect to hydraulic 6-DOF parallel manipulator with heavy payload, the system gravity, the uppermost turbulence to control system for slow motion, results in large steady and dynamic errors in gravitational direction. Therefore, the design and realization of proportional plus derivative controller with dynamic gravity compensation in hydraulic 6-DOF parallel manipulator is of critical importance for improving system control performance of hydraulic driven 6-DOF parallel manipulator especially for the parallel manipulator with heavy payload.

Parallel manipulator has been extensively studied due to its high force-to-weight ratio and widespread application [4]. 6-DOF parallel manipulator is named Stewart platform after Stewart illustrated the use of such parallel structure [5], it is also referred to as Gough-platform who presented the practical use of such a system [6]. Hunt [7] researched the kinematics of parallel manipulators based on screw theory and enumerated promising kinematics structures. Do and Yang [8] used the Newton-Euler approach to solve the inverse dynamics for Stewart platform assuming the joints as frictionless and legs asymmetrical. The control strategies for parallel manipulator may be largely divided into two schemes, joint-space control developed in joint space coordinates [9-11], and workspace control designed based on the workspace coordinates [12-14]. The joint space control scheme can be readily implemented as a collection of multiple, independent single-input single-output control system using data on each actuator length only. A classical proportional plus integral plus derivative control in joint space has been employed in industry, but it does not always guarantee a high performance for parallel robots [15]. This novel joint space control approaches have been proposed to improve control performance by rejecting the uncertainty and nonlinear effects in motion equations. Kim proposed a robust nonlinear control scheme in joint space for a hydraulic parallel system based on Lyapunov redesign method [10], yet the pressure closed loop control is hard to implemented for real hydraulic system due to the effect of pipeline pressure transient and frication force. Nguyen et al [11] developed a joint-space adaptive control scheme applied to an electromechanically driven Stewart platform using Lyapunov direct method. Su presented a robust auto-disturbance rejection controller in joint space for 6-DOF parallel manipulator [16]. Kim et al [12] discussed robust nonlinear task space control with a friction estimator for dynamoelectric Gough-Stewart platform. Burdet et al [17] investigated a nonlinear controller with dynamic compensation which depended on system state and velocity of 6-DOF parallel manipulator. Noriega et al [18] presented a neural network

control scheme and showed its superiority over a kinematics control. Kim et al [19] researched and applied a high speed tracking control for 6-DOF electric driven Stewart platform using an enhanced sliding mode control approach. Cervantes et al [20] studied tracking problem of robot manipulator based on multi-rigid body models with revolute joints via PID control. Although the above advanced model-based control strategies are effective for 6-DOF parallel manipulator, the characteristics of hydraulic driven system is not taken into account. Davliakos et al [21] developed operational error joint feedback control scheme embedding the forward kinematics in the feedback control loop for 6-DOF electrohydraulic Parallel manipulator platforms. However, only simulation is investigated for the model-based control scheme. Besides, the influences of dynamical gravity to system control performance are not analyzed and attracted attention for the proposed controller.
In this paper, a proportional plus derivative controller with dynamic gravity compensation (PDGC) is developed to improve the control performance including steady and dynamic precision via compensating steady state errors and reducing dynamic errors for a 6-DOF hydraulic driven parallel manipulator with symmetric joint locations. This paper begins with a practical strategy to obtain 6-DOF hydraulic driven Gough-Stewart platform essential to the developed controller. The dynamics models of the 6-DOF platform system are built using Kane method, considering the Gough-Stewart platform as 13 rigid bodies, and the hydraulic driven system are established in terms of hydromechanics theory. The desired actuator length is calculated by a closed-solution inverse kinematics, and the system states of 6-DOF Gough-Stewart platform are obtained by a numerical forward kinematics, the forward kinematics and inverse kinematics models are described with Newton-Raphson method and closed-form solution, respectively. The proportional plus derivative with dynamics compensation control scheme is gained, combing the kinematics control and inverse dynamics method, the proposed controller employs rigid body and actuation dynamic and yields the input current vector of the servovalve, the dynamic gravity term including the gravity of platform, load and hydraulic cylinders is used to compensate the influence of gravity of 6-DOF Gough-Stewart platform, and the decoupling of hydraulic system is implemented by local velocity compensation in inner control loop. The performance including stability, precision and robustness of the proposed controller is analyzed in theory and simulation. The proportional plus derivative with dynamic compensation control scheme is studied to improve the performance of control system for 6-DOF hydraulic driven Gough-Stewart platform.

2. System model

The kinematics of 6-DOF Gough-Stewart platform has been studied extensively [22, 23]. Therefore, the kinematics models of 6-DOF Gough-Stewart are briefly described in the paper. Fig.1 depicts the configuration of the 6-DOF Gough-Stewart; Fig.2 explains the two Cartesian coordinate systems; the {**B**} coordinate system is the body coordinate system fixed to the movement platform, while the {**L**} coordinate system is the base coordinate system for the inertial frame. The linear motions denotes as surge (q_1), sway (q_2), and heave (q_3) are along the X_L-Y_L-Z_L axis for base coordinate system, and the angular motions labeled as roll (q_4), pitch (q_5), and yaw (q_6) are Euler angles of platform at X_L, Y_L, Z_L axis. The body coordinate system {**B**} and the base coordinate system {**L**} are superposition in the initial state q_i=0, i=1,…,6.

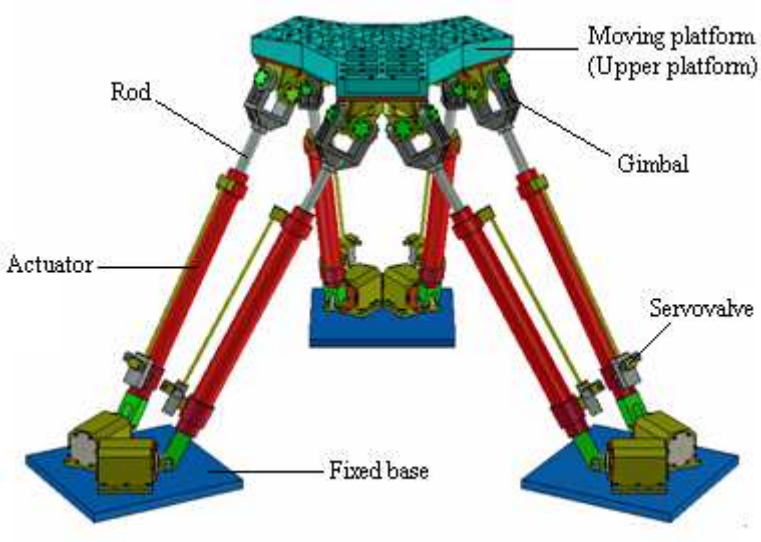

Fig. 1. Configuration of 6-DOF Gough-Stewart platform

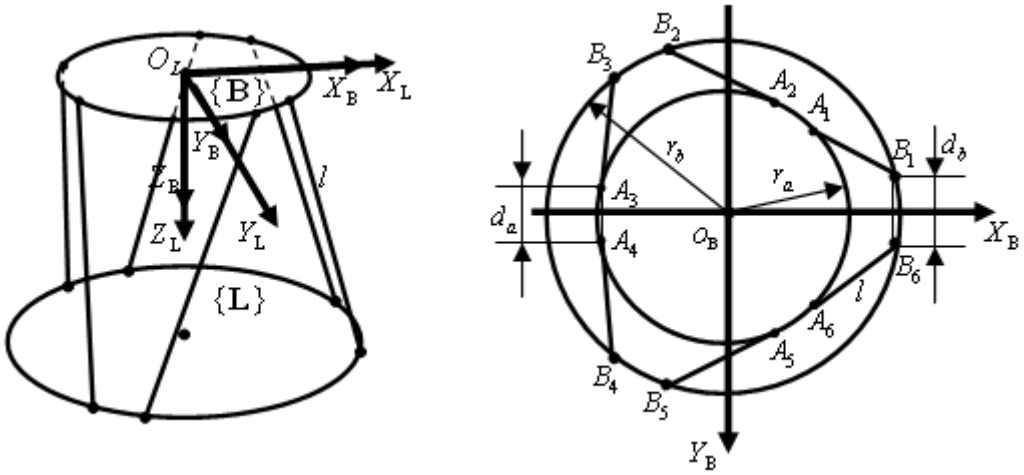

Fig. 2. Definition of the Cartesian coordination systems and vectors in dynamics and kinematics equations of

6-DOF Gough-Stewart platform

For the movement including the linear and angular motions of Gough-Stewart platform, the inverse kinematics model is derived using closed-form solution [22].

$$\widetilde{\mathbf{l}} = (\mathbf{R} \cdot \widetilde{\mathbf{A}} - \widetilde{\mathbf{B}}) + \widetilde{\mathbf{c}} \tag{1}$$

where $\widetilde{\mathbf{l}}$ is a 3×6 actuator length matrix of platform, $\mathbf{R}$ is a 3×3 rotation matrix of transformation from body coordinates to base coordinates, $\widetilde{\mathbf{A}}$ is a 3×6 matrix of upper gimbal points, $\widetilde{\mathbf{B}}$ is a 3×6 matrix of lower gimbal points, and $\widetilde{\mathbf{c}}$ is position 3×1 vector of platform, $\widetilde{\mathbf{c}} = (q_1, q_2, q_3)^{\mathrm{T}}$. The rotation matrix under Z-Y-X order is given by

$$\mathbf{R} = \begin{bmatrix} \cos q_5 \cdot \cos q_6 & \cos q_6 \cdot \sin q_5 \cdot \sin q_4 - \sin q_6 \cdot \cos q_4 & \sin q_6 \cdot \sin q_4 + \cos q_6 \cdot \sin q_5 \cdot \cos q_4 \\ \sin q_6 \cdot \cos q_5 & \cos q_6 \cdot \cos q_4 + \sin q_6 \cdot \sin q_5 \cdot \sin q_4 & \sin q_6 \cdot \sin q_5 \cdot \cos q_4 - \cos q_6 \cdot \sin q_4 \\ -\sin q_5 & \cos q_5 \cdot \sin q_4 & \cos q_5 \cdot \cos q_4 \end{bmatrix} \tag{2}$$

The forward kinematics is used to solve the output state of platform for a measured length vector of actuators; it is formulated with Newton-Raphson method [23].

$$\widetilde{\mathbf{\Theta}}_{j+1} = \widetilde{\mathbf{\Theta}}_j + \mathbf{J}_{l,\widetilde{\Theta}}^{-1} \cdot (\widetilde{\mathbf{l}}_0 - \widetilde{\mathbf{l}}_j) \tag{3}$$

where $\widetilde{\mathbf{\Theta}}$ is a 6×1 state vector of the platform generalized coordinates, $\widetilde{\mathbf{\Theta}} = (q_1, q_2, q_3, q_4, q_5, q_6)^{\mathrm{T}}$, j is the iterative numbers, $\widetilde{\mathbf{l}}_0$ is the initial measured length 6×1 vector of actuator of the platform, $\widetilde{\mathbf{l}}_j$ is the 6×1 solving actuator vector during the iterative calculation, $\mathbf{J}_{l,\widetilde{\Theta}}$ is a Jacobian 6×6 matrix, which is one of the most important variables in the Gough-Stewart platform, relating the body coordinates to be controlled and used as basic model coordinates, and the actuator lengths, which can be measured.

The dynamic model for motion platform as a rigid body can be derived using Newton-Euler and Kane method [24, 25].

$$\widetilde{\boldsymbol{\tau}} + \widetilde{\mathbf{G}}(\widetilde{\mathbf{\Theta}}) = \widetilde{\mathbf{M}}(\widetilde{\mathbf{\Theta}}) \cdot \ddot{\mathbf{\Theta}} + \widetilde{\mathbf{V}}(\widetilde{\mathbf{\Theta}}, \dot{\mathbf{\Theta}}) \cdot \dot{\mathbf{\Theta}} \tag{4}$$

where $\widetilde{\mathbf{M}}(\widetilde{\mathbf{\Theta}})$ is a 6×6 mass matrix, $\widetilde{\mathbf{V}}(\widetilde{\mathbf{\Theta}}, \dot{\mathbf{\Theta}})$ is a 6×6 matrix of centrifugal and Coriolis terms, $\widetilde{\mathbf{G}}(\widetilde{\mathbf{\Theta}})$ is a 6×1 vector of gravity terms, see Appendix A, $\widetilde{\boldsymbol{\tau}}$ is a 6×1 vector of generalized applied forces, $\dot{\mathbf{\Theta}}$ is a 6×1 velocity vector, which is given by

$$\dot{\mathbf{\Theta}} = (\dot{\widetilde{\mathbf{c}}} \quad \widetilde{\boldsymbol{\omega}})^{\mathrm{T}} \tag{5}$$

where $\widetilde{\boldsymbol{\omega}}$ is a 3×1 angular velocity vector in base coordinate system, $\widetilde{\boldsymbol{\omega}} = (\omega_x \quad \omega_y \quad \omega_z)^{\mathrm{T}}$. Note that $\dot{\mathbf{\Theta}} \neq \dot{\widetilde{\mathbf{\Theta}}}$.

The applied forces $\boldsymbol{\tau}$ can be transformed from mechanism actuator forces, which is given by

$$\widetilde{\boldsymbol{\tau}} = \mathbf{J}_{l,\widetilde{\Theta}}^{\mathrm{T}} \cdot \mathbf{F}_{\mathrm{a}} \tag{6}$$

where $\mathbf{F}_a$ is a 6×1 vector representing actuator forces, $\mathbf{F}_{\mathrm{a}} = (f_{\mathrm{a1}} \quad f_{\mathrm{a2}} \quad \cdots \quad f_{\mathrm{a6}})^{\mathrm{T}}$, f_{ai} (i=1,…,6) is actuator output force.
The rotation of actuator around itself is ignored, thus the dynamic model for each hydraulic actuator (piston rod and cylinder) using Newton-Euler and Kane method is described as

$$(\mathbf{J}_{\mathrm{uc},ai}\mathbf{J}_{ai,\widetilde{\Theta}})^{\mathrm{T}} m_{\mathrm{u}} \cdot \mathbf{g} + (\mathbf{J}_{\mathrm{tc},ai}\mathbf{J}_{ai,\widetilde{\Theta}})^{\mathrm{T}} m_{\mathrm{t}} \cdot \mathbf{g} = \overline{\mathbf{F}}_{\mathrm{i}} \tag{7(a)}$$

$$\begin{aligned}\overline{\mathbf{F}}_{\mathrm{i}} = {} & (\mathbf{J}_{\mathrm{uc},ai}\mathbf{J}_{ai,\widetilde{\Theta}})^{\mathrm{T}} m_{\mathrm{u}} \cdot \overline{\mathbf{v}}_{\mathrm{uc}} + (\mathbf{J}_{\mathrm{uc},ai}\mathbf{J}_{ai,\widetilde{\Theta}})^{\mathrm{T}} (\mathbf{I}_{\mathrm{a}}\dot{\overline{\boldsymbol{\omega}}}_i + \widetilde{\boldsymbol{\omega}} \times \mathbf{I}_{\mathrm{a}}\overline{\boldsymbol{\omega}}_i) + \mathbf{J}_{\mathrm{tc},ai}\mathbf{J}_{ai,\widetilde{\Theta}})^{\mathrm{T}} m_{\mathrm{t}} \cdot \overline{\mathbf{v}}_{\mathrm{tc}} \\ & + (\mathbf{J}_{\mathrm{tc},ai}\mathbf{J}_{ai,\widetilde{\Theta}})^{\mathrm{T}} (\mathbf{I}_{\mathrm{b}}\dot{\overline{\boldsymbol{\omega}}}_i + \widetilde{\boldsymbol{\omega}} \times \mathbf{I}_{\mathrm{b}}\overline{\boldsymbol{\omega}}_i)\end{aligned} \tag{7(b)}$$

where $\mathbf{J}_{\mathrm{uc},ai}, \mathbf{J}_{\mathrm{tc},ai}$ are 3×3 Jacobian matrix, $, \mathbf{J}_{ai,\widetilde{\Theta}}$ is 3×6 Jacobian matrix, m_{u} is the mass of piston rod of a actuator, m_{t} is the mass of cylinder of a actuator, $\overline{\boldsymbol{\omega}}_i$ is the angular velocity of actuator relative to relevant lower gimbal point, $\overline{\mathbf{v}}_{\mathrm{uc}}, \overline{\mathbf{v}}_{\mathrm{tc}}$ are the linear velocity of the mass center of piston rod and cylinder, respectively, $\mathbf{I}_{\mathrm{a}}, \mathbf{I}_{\mathrm{b}}$ are the inertia of piston rod and cylinder, respectively, **g** is acceleration vector of gravity, **g**=(0 0 g)$^{\mathrm{T}}$.
Combining Eqs.(4), (5),(6) and (7), the dynamics model of 6-DOF Gough-Stewart platform as thirteen rigid body is obtained with Kane method, given by

$$\widetilde{\boldsymbol{\tau}} + \mathbf{G}^*(\widetilde{\boldsymbol{\Theta}}) = \mathbf{M}^*(\widetilde{\boldsymbol{\Theta}}) \cdot \ddot{\boldsymbol{\Theta}} + \mathbf{V}^*(\widetilde{\boldsymbol{\Theta}}, \dot{\boldsymbol{\Theta}})\dot{\boldsymbol{\Theta}} \tag{8}$$

where, $\mathbf{M}^*(\widetilde{\boldsymbol{\Theta}})$ is a mass matrix, $\mathbf{V}^*(\widetilde{\boldsymbol{\Theta}}, \dot{\boldsymbol{\Theta}})$ is a matrix of centrifugal and Coriolis terms, $\mathbf{G}^*(\widetilde{\boldsymbol{\Theta}})$ is a vector of gravity terms, see Appendix B.
The hydraulic systems are studied in depth for symmetrical servovalve and actuator [26], it is assumed that Coulomb frictions are zero (Coulomb friction $F_{\mathrm{ci}} << B_c\dot{l}_i$, not zero, practically) the hydraulic system mathematical models of symmetric and matched servovalve and symmetrical actuator are given as

$$q_{\mathrm{L}i} = C_{\mathrm{d}} \cdot w \cdot x_{\mathrm{v}i}\sqrt{\frac{1}{\rho}(p_{\mathrm{s}} - \mathrm{sign}(x_{\mathrm{v}i})p_{\mathrm{L}i})} \tag{9}$$

$$q_{\mathrm{L}i} = A \cdot \dot{l}_i + C_{\mathrm{te}} \cdot p_{\mathrm{L}i} + \frac{V_{\mathrm{t}}}{4E}\dot{p}_{\mathrm{L}i} \tag{10}$$

$$A \cdot p_{\mathrm{L}i} = f_{ai} + f_{fi} \tag{11}$$

where $q_{\mathrm{L}i}$ is load flow of the i^{th} hydraulic actuator, w is area grads, $x_{\mathrm{v}i}$ is position of the i^{th} servovalve, ρ is fluid density, p_s is supply pressure of servosystem, p_{Li} is load pressure of the i^{th} actuator, A is effective acting area of piston, C_{te} is the leakage coefficient, V_{t} is actuator cubage, E is bulk modulus of fluid, l_i is the length of the i^{th} actuator, C_{d} is flow

coefficient, f_{fi} is joint space friction force in the i^{th} actuator. A number of methods can be used to model the friction $\mathbf{F}_f$ [21, 27]. A widely method for modeling friction as

$$\mathbf{F}_f(\dot{l}) = \mathbf{F}_v(\dot{l}) + \mathbf{F}_c(\dot{l}) + \mathbf{F}_s \tag{12}$$

where $\mathbf{F}_f$ is total friction vector, $\mathbf{F}_f = [f_{f1} \quad \cdots \quad f_{f6}]^{\mathrm{T}}$, $\mathbf{F}_v$, $\mathbf{F}_c$ and $\mathbf{F}_s$ are the viscous, Coulomb and static friction vector, respectively, with elements

$$f_{vi}(\dot{l}_i) = \begin{cases} B_c \dot{l}_i, & \dot{l}_i \neq 0 \\ 0, & \dot{l}_i = 0 \end{cases} \qquad i=1,2,\ldots,6 \tag{13}$$

$$f_{ci}(\dot{l}_i) = \begin{cases} f_{c0,i}\,\mathrm{sign}(\dot{l}_i), & \dot{l}_i \neq 0 \\ 0, & \dot{l}_i = 0 \end{cases} \qquad i=1,2,\ldots,6 \tag{14}$$

$$f_{si}(\dot{l}_i) = \begin{cases} f_{\mathrm{ext},i}, & |f_{\mathrm{ext},i}| < f_{s0,i} \quad \dot{l}_i = 0, \ddot{l}_i = 0 \\ f_{s0,i}\,sign(\dot{l}_i), & |f_{\mathrm{ext},i}| > f_{s0,i} \quad \dot{l}_i = 0, \ddot{l}_i \neq 0 \\ 0, & \dot{l}_i \neq 0 \end{cases} \quad i=1,2,\ldots,6 \tag{15}$$

where B_c is viscous damping coefficient, $f_{c0,i}$ is the element of Coulomb friction, $f_{\mathrm{ext},i}$ is the external force element, $f_{s0,i}$ is the breakaway force element.

3. Control design

In this section, the inverse dynamic methodology [20] is adopted to derive a proportional plus derivative controller with dynamic gravity compensation for 6-DOF hydraulic driven Gough-Stewart platform in the case in which the system parameters are known, the PDGC control scheme are described in Fig.3.

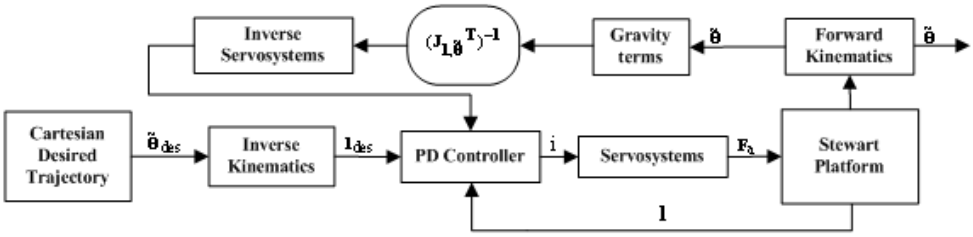

Fig. 3. Control block diagram for PDGC

The PDGC controller considered the dynamic characteristic of parallel manipulator embedded the forward kinematics, dynamic gravity terms and inverse of transfer function from the input position of servovalve to the output force of actuator and Jacobian matrix $(\mathbf{J}_{l\Theta}{}^{\mathrm{T}})^{-1}$ in inverse of transpose form in inner control loop. It is should be noted that

the friction force, zero bias and dead zone of servovalve also affect the steady and dynamic precision as well as system gravity. However, the valve with high performance index may be chosen to avoid the effect of dead zone of control valve. In fact, the dead zone of servovalve in hydraulic system is very small, which can achieve 0.01mm even a general servovalve. The zero bias of servovalve may be measured and compensated for control system. For large hydraulic parallel manipulator with heavy payload, the system gravity is much more that the maximal friction even that no payload exist in hydraulic 6-DOF parallel manipulator. Therefore, the dynamical gravity, the most chief influencing factor of steady precision, and viscous friction is taken into account for designing of the developed control scheme without considering Column and static friction in this paper. Besides, the classical PID is widely applied in hydraulic 6-DOF parallel manipulator in practice, then the considered system gravity is associated with PID control to improve the steady and dynamic precision without destroy the steadily of the original control system.
The nature frequency of servovalve is higher than the mechanical and hydraulic commix system, so Eqs.(9) can be linearized using Taylor formulation, rewritten by

$$q_{Li} = K_q x_{vi} - K_c p_{Li} \tag{16}$$

With Eqs.(10)-(13), (10) and (11) are rewritten in the form of La-transformation.

$$Q_{Li} = A \cdot sL_i + C_{te} \cdot P_{Li} + \frac{V_t}{4E} \cdot sP_{Li} \tag{17}$$

$$A \cdot P_{Li} = B_c \cdot sL_i + F_{ai} \tag{18}$$

The input current of servovalve is direct proportion to position of servovalve, so

$$i_i = K_0 x_{vi} \tag{19}$$

where, K_0 is a constant.

Substituting the Eqs.(16),(17) and (19) in Eqs.(17), the output of inverse servosystem, given by

$$\widetilde{I}_i = \{\frac{1}{A}(F_{ai} + B_c \cdot sL_i)(K_c + C_{te} + \frac{V_t}{4E}s) + A \cdot sL_i\} \cdot \frac{K_0}{K_q} \tag{20}$$

where,

$$F_{ai} = \{(\mathbf{J}_{l,\widetilde{\Theta}}{}^{\mathrm{T}})^{-1} \cdot \mathbf{G}^*(\widetilde{\mathbf{\Theta}})\}_i$$

The developed controller is extended to model-based control scheme allowing tracking of the reference inputs for platform. Desired position vector of hydraulic cylinders and actual position vector of hydraulic cylinders are used as input commands of the controller, and the controller provides the current sent to the servovale, the closed-loop control law can be shown as

$$u_i = f_i = (K_0 k_p e_i + K_0 k_d \dot{e}_i - \widetilde{i}_i) \cdot G \tag{21}$$

where u_i is the output of actuator, k_p and k_d are control gain of system, G is the transfer function of the output current of servovalve to the actuator output forces, e is actuator length error of the platform, e_i=l_{ides}-l_i, l_{ides} is the desired hydraulic cylinders length, l_i is the feedback hydraulic cylinder length.
Using Eqs.(20), the Eqs.(21) can be rewritten by

$$\mathbf{u} = (k_p \mathbf{e} + k_d \dot{\mathbf{e}}) K_0 \cdot G - (\mathbf{J}_{l,\tilde{\Theta}}{}^{\mathrm{T}})^{-1} \cdot \mathbf{G}^*(\tilde{\mathbf{\Theta}}) \tag{22}$$

where,

$$\mathbf{u} = (u_1, u_2, ..., u_6)^{\mathrm{T}},$$
$$\mathbf{e} = (e_1, e_2, ..., e_6)^{\mathrm{T}}.$$

Combining Eqs.(8), (22), an system equation of the 6-DOF parallel manipulator with PDGC controller can be obtained, which can be shown as

$$\mathbf{J}_{l,\tilde{\Theta}}{}^{\mathrm{T}} \cdot \mathbf{u} + \mathbf{G}^*(\tilde{\mathbf{\Theta}}) = \mathbf{M}^*(\tilde{\mathbf{\Theta}}) \cdot \ddot{\mathbf{\Theta}} + \mathbf{V}^*(\tilde{\mathbf{\Theta}}, \dot{\mathbf{\Theta}}) \dot{\mathbf{\Theta}} \tag{23}$$

According to Eqs.(23), the system error dynamics for pointing control can be written as

$$\mathbf{M}^*(\tilde{\mathbf{\Theta}}) \cdot \ddot{\mathbf{e}} + [\mathbf{V}^*(\tilde{\mathbf{\Theta}}, \dot{\mathbf{\Theta}}) + k_d] \cdot \dot{\mathbf{e}} + k_p \mathbf{e} = 0 \tag{24}$$

The Lyapunov function is chosen for PDGC control scheme, and the rest of stability proof is identical to the one in [28].

$$V = \frac{1}{2} \dot{\mathbf{e}}^{\mathrm{T}} \mathbf{M}^*(\tilde{\mathbf{\Theta}}) \dot{\mathbf{e}} + \frac{1}{2} \mathbf{e}^{\mathrm{T}} k_p \mathbf{e} \tag{25}$$

The error term $(\dot{\mathbf{e}}, \ddot{\mathbf{e}})$ and the generalized coordinates term $(\dot{\mathbf{\Theta}}, \ddot{\mathbf{\Theta}})$ in Eqs.(24) are zero in steady state, so the steady state error vector $\mathbf{e}$ converge to zero, the actual actuator length $\mathbf{l}$ can converge asymptotical to the desired actuator length $\mathbf{l}_{des}$ without errors.

4. Experiment results

The control performance including steady state precision, stability and robustness of the proposed PDGC is evaluated on a hydraulic 6-DOF parallel manipulator in Fig.4 via experiment, which features (1) six hydraulic cylinders, (2) six MOOG-G792 servo-valves, (3) hydraulic pressure power source, (4) signal converter and amplifier, (5) D/A ACL-6126 board, (6) A/D PCL-816/818 board, (7) position and pressure transducer, (8) a real-time industrial computer for real-time control, and (9) a supervisory control computer. The control program of the parallel manipulator is programmed with Matlab/Simulink and compiled to gcc code executed on target real-time computer with QNX operation system using RT-Lab. The sampling time for the control system is set to 1 ms, and the parameters of the hydraulic 6-DOF parallel manipulator are summarized in Table 1.

Parameters	Value
Maximal/Maximal stroke of cylinder, l_{min}/l_{max} (m)	-0.37/0.37
Initial length of cylinder, l_0 (m)	1.830
Upper joint spacing, d_u (m)	0.260
Lower joint spacing, d_d (m)	0.450
Upper joint radius, R_u (m)	0.560
Lower joint radius, R_d (m)	1.200
Mass of upper platform and payload, m_p (Kg)	2940
Moment of inertia of upper platform and payload, I_{xx}, I_{yy}, I_{zz} (Kg·m^2)	217.37, 217.37, 266.75

Table 1. Parameters of hydraulic 6-DOF parallel manipulator

Fig. 4. Experimental hydraulic 6-DOF parallel manipulator

The spatial states of parallel manipulator are critical to determine the control input for compensating system gravity, turbulence for the control system of hydraulic 6-DOF parallel manipulator. Fortunately, the real-time forward kinematics for estimating system states has been investigated and implemented with high accuracy (less than 10^{-7}m) and sample 1-2ms [29]. It is should be noted that the steady state error in principle of control system mainly results from system gravity of the 6-DOF parallel manipulator especially for hydraulic parallel manipulator with heavy payload, even though the friction always exists in the system under position control, since the gravity of the payload and upper platform is much more than friction.

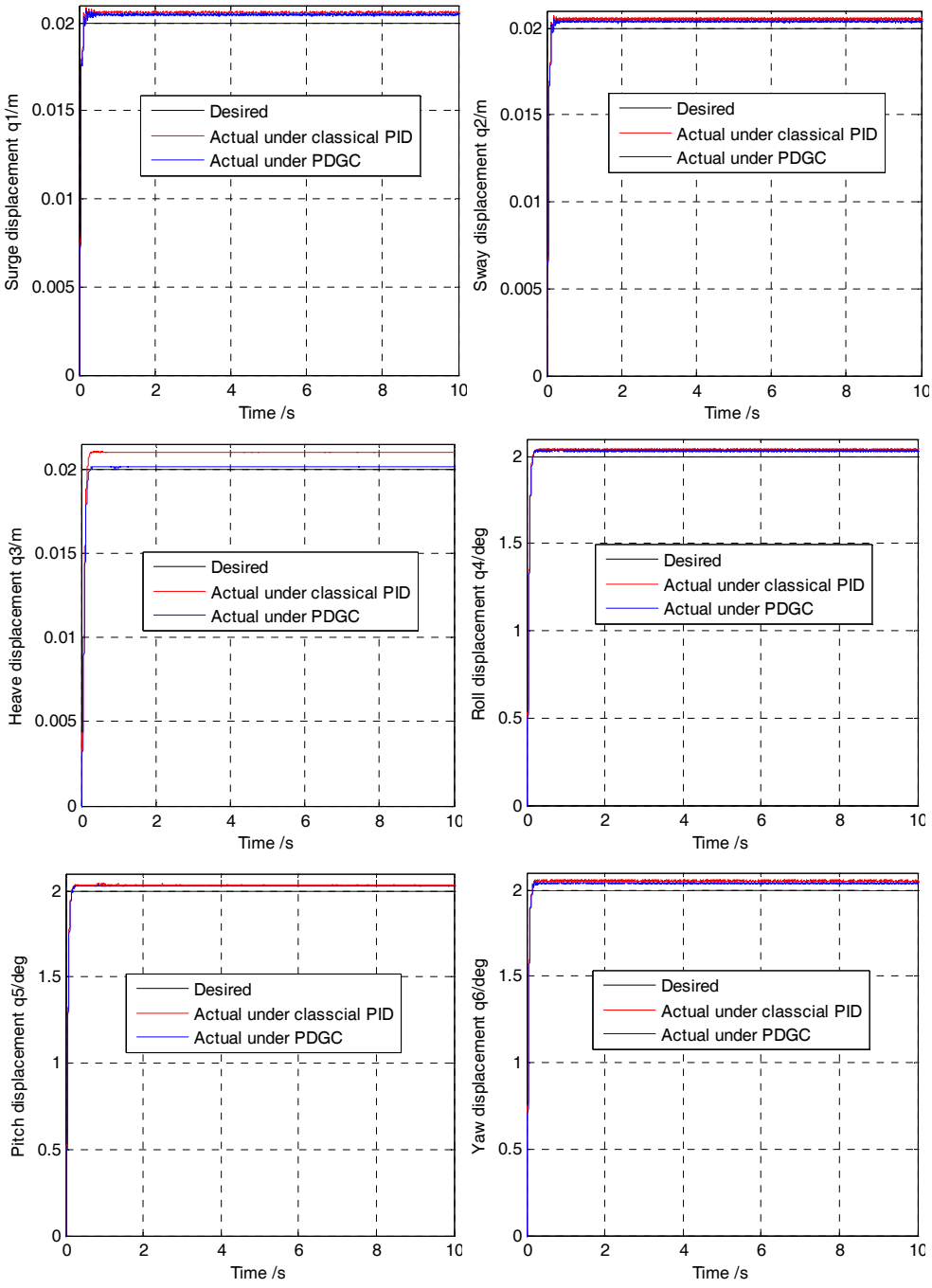

Fig. 5. Responses to desired step trajectories of classical PID and PDGC controller

With online forward kinematics available, the proposed PDGC strategy is implemented in a real 6-DOF hydraulic parallel manipulator. The classical PID control scheme is also applied to the parallel manipulator as benchmarking for that the classical PID control is a typical control strategy in theory and practice, particularly in industrial hydraulic 6-DOF parallel manipulator with heavy payload. It is should be noted that the proposed PDGC control is an improved PID control with dynamical gravity compensation to improve the control performance involving both steady and dynamic precision of hydraulic 6-DOF parallel manipulator, the control strategy with gravity compensation also may be incorporated with other advanced control scheme to derive better control performance. The classical PID gain Kp is experimental tuned to 40, which is identical with the proposed PDGC gains. All six DOFs step signals (Surge: 0.02m, Sway: 0.02m, Heave: 0.02m, roll: 2deg, Pitch: 2deg, Yaw: 2deg) are applied to the actual control system, respectively. Fig.5 shows the responses to the desired step trajectory of experimental hydraulic parallel manipulator.

As shown in Fig.5, the PDGC control scheme can respond to the desired step trajectories promptly and steadily in all DOFs. Moreover, the proposed PDGC shows superior control performance in steady precision to those of the classical PID control along all six DOFs directions. The maximal steady state error is 0.41mm in linear motions and 0.04deg in angular motions under the PDGC, 1.01mm in linear motions and 0.052deg in angular motions under the classical PID. The maximal steady state error chiefly influenced by system gravity appeared in heave direction motion for all 6 DOFs motions under the classical PID control, which was compensated via the proposed PDGC control, depicted in Fig.6. Compared with the PDGC controller, the maximal steady state error in angular motions presented in yaw direction under classical PID control is also shown in Fig.6. The steady state error is 0.1mm in heave and 0.03deg in yaw with PDGC, 1.01mm in heave and 0.052deg in yaw with classical PID. Additionally, the responses to the step trajectories also illustrate that the control system, both PDGC and classical PID control, is steady.

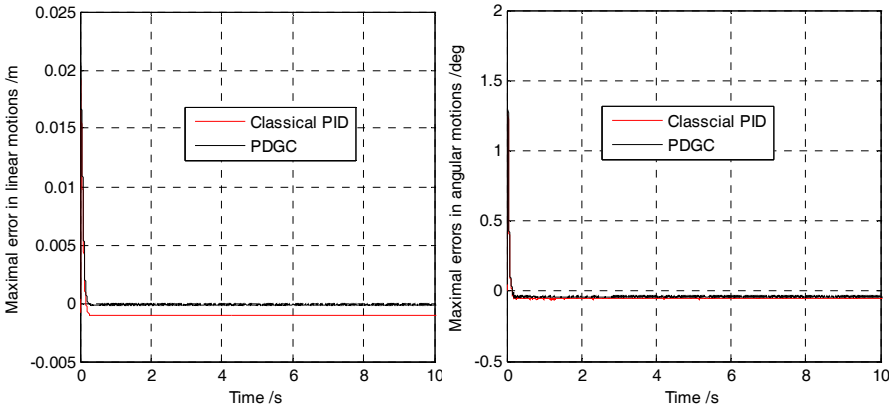

Fig. 6. The maximal errors of PDGC and classical PID controller in position and orientation

With a view of evaluating the dynamic control performance of the PDGC, the desired sinusoidal signals are inputted to the hydraulic parallel manipulator. Under sinusoidal inputs along six directions: surge (0.01m/1Hz), sway (0.01m/2Hz), heave (0.01m/1Hz), roll (1deg/1Hz), pitch (1deg/2Hz), and yaw (1deg/1Hz), the trajectory tracking for the PDGC control and the classical PID control scheme are shown in Fig. 7.

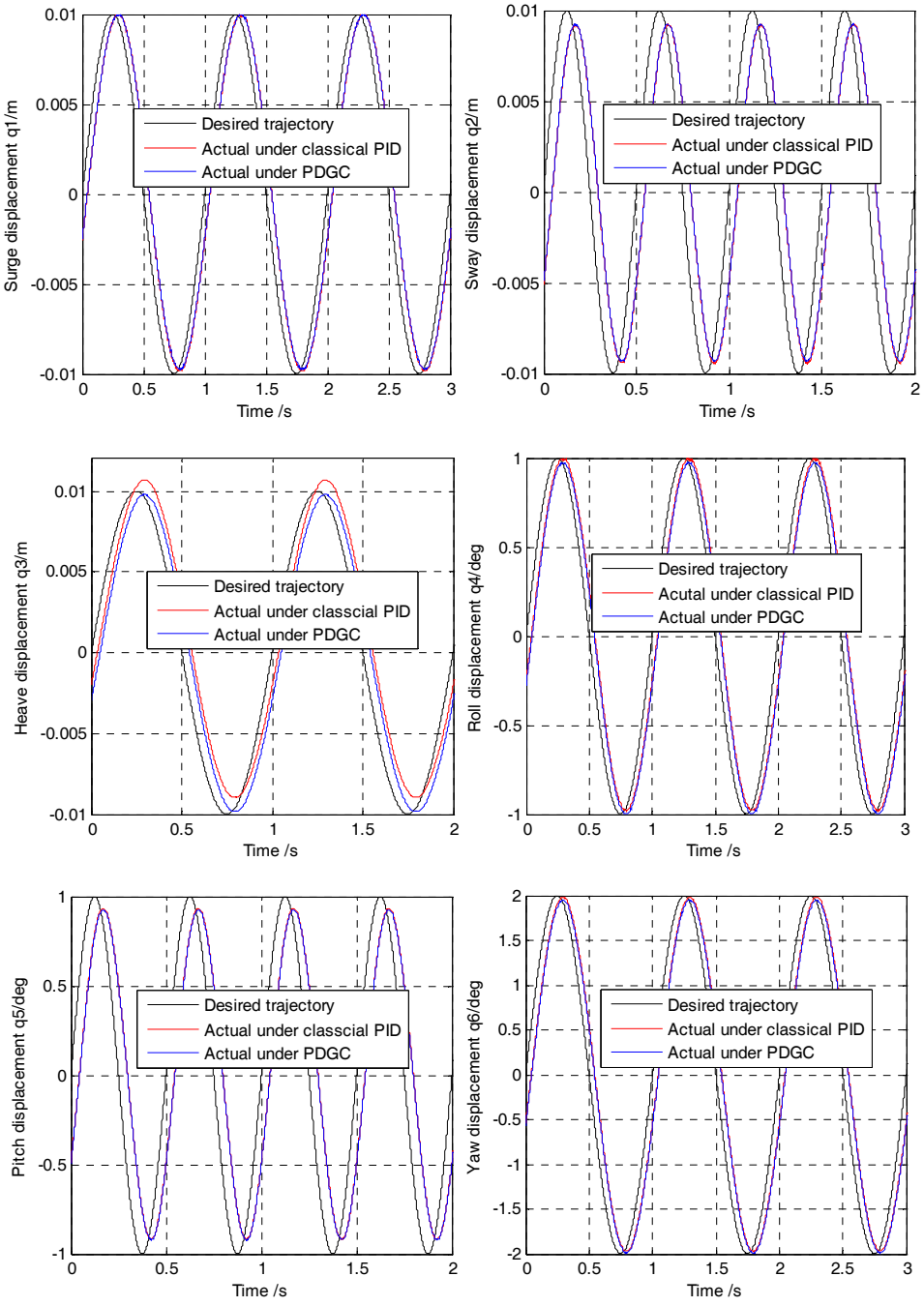

Fig. 7. Responses to desired sinusoidal trajectories of classical PID and PDGC controller

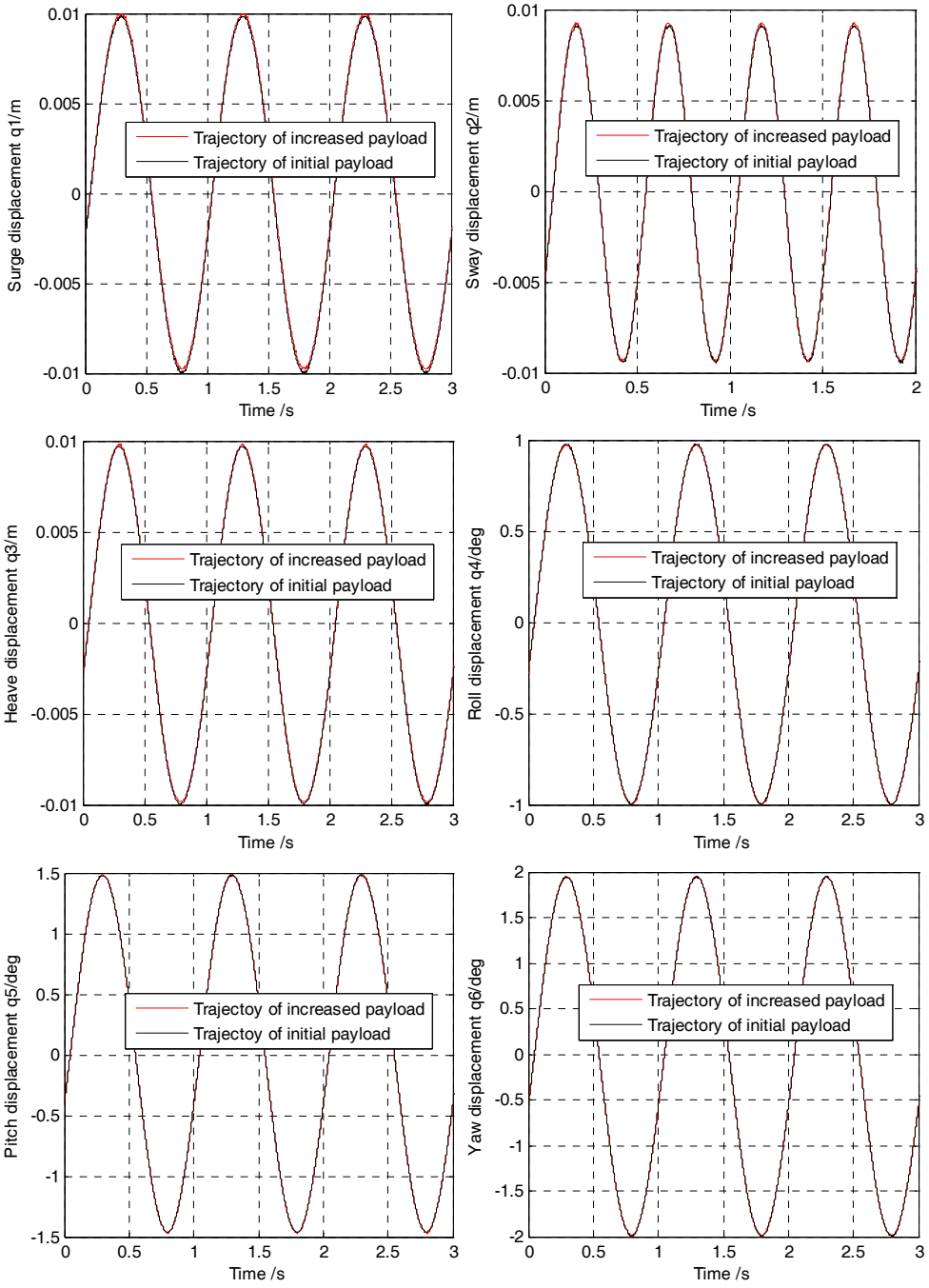

Fig. 8. Experimental results for different mass of payload

As can be deduced form Fig. 5-7, the hydraulic 6-DOF Gough-Stewart platform with PDGC, lead the systems to the desired location with smaller steady state error neglected in large hydraulic 6-DOF parallel manipulator, while the classical proportional plus integral plus derivative control scheme exist large steady state errors in the system, and the PDGC control system can implement trajectory tracking of sine wave with excellent performance in all DOFs motions, which is better than classical proportional plus integral plus derivative controller especially in heave direction motion.
The influence of platform load variable during the motion of 6-DOF parallel manipulator and the robustness of the controller can be illustrated by applied the controller to the system in the case of the platform load increase by 12%, the experimental results are shown in the Fig.8.

Comparison of results demonstrate that the maximal amplitude fading with increased mass of payload is 0.644dB in linear motions (q1, q2, q3), 0.154dB in angular motions (q4, q5, q6), and it is 0.661dB in linear motions and 0.153dB in angular motions for initial mass of payload, the maximal phase delay of PDGC controller with 112% of initial mass is 0.14rad relative to initial mass in linear motions, while it is 0.023rad phase delay than it was with initial mass in angular motions. Consequently, the proposed control still has excellent performance (robustness) with incorrect mass of payload which is 112% of initial mass. Moreover, the experimental results display that the proposed PDGC control scheme can improve the steady precision and reduce system dynamic errors of hydraulic 6-DOF parallel manipulator even 12% uncertainty exists in gravity, especially for 6-DOF parallel manipulator with heavy payload.

5. Conclusions

In this paper, a proportional plus derivative control with dynamic gravity compensation is studied for 6-DOF parallel manipulator. The system models are derived, including the dynamics model of 6-DOF Gough-Stewart platform and actuators using Kane method and the forward kinematics with Newton-Raphson method and the inverse kinematics in closed-form solution, and the hydraulic systems based on hydromechanics theory. The control law of proportional plus derivative control with dynamic gravity compensation is developed in the paper, the inner loop feedback controller employed dynamic gravity term, forward kinematics and Jacobian matrix and yield servovalve currents, and the dynamics of hydraulic systems are decoupled by local velocity compensation in inverse servosystem, the outer loop implement the position control of actuator length. The direct estimation method for the system states required in the proposed control based on the forward kinematics are employed in order to realize the control scheme in the base coordinate systems instead of the state observer with the actuator length output. The performances with respect to stability, precision and robustness are analyzed. The theoretical analysis and simulation results demonstrate that the proposed controller represent excellent performance for the 6-DOF hydraulic driven Gough-Stewart platform, it is stable, the steady state errors of the system due to gravity of the systems are converge asymptotically to zero, and the controller reveal superexcellent robustness. Furthermore, the effective PDGC control for the hydraulic 6-DOF parallel manipulator with heavy payload is obtained in this paper; it can not only be used in hydraulic driven 6-DOF parallel manipulator for improving classical PID control

performance, but also can be associated with other advanced control scheme to get better control performance and applied in other systems.

Acknowledgements

This research was supported by 921 Manned Space Project from China Academy of Space Technology and Self-Planned Task (No.SKLRS200803B) of State Key Laboratory of Robotics and System (HIT). The authors would like to thank CAST, HIT, Prof S. J. Li of Department of Mechanical and Electrical Engineering, Harbin Institute of Technology, and to thank the Editor, Associate Editors, and anonymous reviewers for their constructive comments.

Appendix A.

The 6×6 mass matrix $\widetilde{\mathbf{M}}(\widetilde{\boldsymbol{\Theta}})$, 6×6 centrifugal and Coriolis matrix $\widetilde{\mathbf{V}}(\widetilde{\boldsymbol{\Theta}},\dot{\boldsymbol{\Theta}})$, and 6×1 vector of gravity terms $\widetilde{\mathbf{G}}(\widetilde{\boldsymbol{\Theta}})$ in Eqs.(4) are given by

$$\widetilde{\mathbf{M}}(\widetilde{\boldsymbol{\Theta}}) = \begin{bmatrix} m_{\mathrm{p}}\mathbf{I}_{\mathrm{e}} & 0 \\ 0 & \mathbf{I}_L \end{bmatrix} \tag{A.1a}$$

$$\widetilde{\mathbf{V}}(\widetilde{\boldsymbol{\Theta}},\dot{\boldsymbol{\Theta}}) = \begin{bmatrix} 0_{3\times 3} & 0 \\ 0 & \boldsymbol{\Omega}\cdot\mathbf{I}_L \end{bmatrix} \tag{A.1b}$$

$$\widetilde{\mathbf{G}}(\widetilde{\boldsymbol{\Theta}}) = \begin{bmatrix} 0 & 0 & g & 0 & 0 & 0 \end{bmatrix}^{\mathrm{T}} \tag{A.1c}$$

where $\mathbf{I}_{\mathrm{e}}$ is unit 3×3 matrix, $\mathbf{I}_{\mathrm{L}}$ is a 3×3 inertia matrix of upper platform in base coordinates system, m_{p} is the mass of upper platform.

$$\mathbf{I}_{\mathrm{e}} = \begin{bmatrix} 1 & 0 & 0 \\ 0 & 1 & 0 \\ 0 & 0 & 1 \end{bmatrix} \tag{A.2a}$$

$$\mathbf{I}_L = \mathbf{R}\cdot\mathbf{I}_{\mathrm{p}}\cdot\mathbf{R}^{\mathrm{T}} \tag{A.2b}$$

$$\boldsymbol{\Omega} = \begin{bmatrix} 0 & -\omega_z & \omega_y \\ \omega_z & 0 & -\omega_x \\ -\omega_y & \omega_x & 0 \end{bmatrix} \tag{A.2c}$$

where $\mathbf{I}_{\mathrm{p}}$ is 3×3 inertia matrix relative to its symmetrical axis system, $\mathbf{I}_{\mathrm{p}} = \mathrm{diag}\{I_{xx}, I_{yy}, I_{zz}\}$.

Appendix B.

The mass matrix $\mathbf{M}^*(\widetilde{\mathbf{\Theta}})$, matrix of centrifugal and Coriolis term $\mathbf{V}^*(\widetilde{\mathbf{\Theta}},\dot{\mathbf{\Theta}})$, and gravity terms $\mathbf{G}^*(\widetilde{\mathbf{\Theta}})$ in Eqs.(8) are given by

$$\mathbf{G}^*(\widetilde{\mathbf{\Theta}}) = \widetilde{\mathbf{G}}(\widetilde{\mathbf{\Theta}}) + \sum_{i=1}^{6}[(\mathbf{J}_{\mathrm{uc},\mathrm{ai}}\mathbf{J}_{\mathrm{ai},\widetilde{\Theta}})^{\mathrm{T}} m_{\mathrm{u}} \cdot \mathbf{g} + (\mathbf{J}_{\mathrm{tc},\mathrm{ai}}\mathbf{J}_{\mathrm{ai},\widetilde{\Theta}})^{\mathrm{T}} m_{\mathrm{t}} \cdot \mathbf{g}] \tag{B.1a}$$

$$\mathbf{M}^*(\widetilde{\mathbf{\Theta}}) = \widetilde{\mathbf{M}}(\widetilde{\mathbf{\Theta}}) + \sum_{i=1}^{6} \mathbf{J}^{\mathrm{T}}{}_{\mathrm{ai},\widetilde{\Theta}}(\mathbf{M}_{\mathrm{li}} + \mathbf{M}_{\mathrm{agi}})\mathbf{J}_{\mathrm{ai},\widetilde{\Theta}} \tag{B.1b}$$

$$\mathbf{V}^*(\widetilde{\mathbf{\Theta}},\dot{\mathbf{\Theta}}) = \widetilde{\mathbf{V}}(\widetilde{\mathbf{\Theta}},\dot{\mathbf{\Theta}}) + \sum_{i=1}^{6}\{\mathbf{J}^{\mathrm{T}}{}_{\mathrm{ai},\widetilde{\Theta}} \cdot \mathbf{V}_{\mathrm{li}} + \mathbf{V}_{\mathrm{ani}}\} \tag{B.1c}$$

where,

$$\mathbf{M}_{\mathrm{li}} = \mathbf{J}^{\mathrm{T}}{}_{\mathrm{uc},\mathrm{ai}} m_{\mathrm{u}} \mathbf{J}_{\mathrm{uc},\mathrm{ai}} + \mathbf{J}^{\mathrm{T}}{}_{\mathrm{tc},\mathrm{ai}} m_{\mathrm{t}} \mathbf{J}_{\mathrm{tc},\mathrm{ai}} \tag{B.2a}$$

$$\mathbf{M}_{\mathrm{agi}} = \frac{(\mathbf{I}_a + \mathbf{I}_b)}{l_i^{\,2}}(\mathbf{I} - \mathbf{l}_{\mathrm{n}} \cdot \mathbf{l}_{\mathrm{n}}{}^{\mathrm{T}}) \tag{B.2b}$$

$$\mathbf{V}_{\mathrm{li}} = \mathbf{J}^{\mathrm{T}}{}_{\mathrm{uc},\mathrm{ai}} m_{\mathrm{u}} (\mathbf{J}^{\mathrm{T}}{}_{\mathrm{uc},\mathrm{ai}} \dot{\mathbf{J}}_{\mathrm{ai},\widetilde{\Theta}} + \dot{\mathbf{J}}_{\mathrm{uc},\mathrm{ai}} \mathbf{J}_{\mathrm{ai},\widetilde{\Theta}}) \tag{B.2c}$$

$$\mathbf{V}_{\mathrm{ani}} = -\frac{2(\mathbf{I}_a + \mathbf{I}_b)}{l_i^{\,2}}(\mathbf{l}_{\mathrm{ni}}{}^{\mathrm{T}} \cdot \mathbf{J}_{\mathrm{ai},\widetilde{\Theta}} \dot{\mathbf{\Theta}})(\mathbf{I} - \mathbf{l}_{\mathrm{n}} \cdot \mathbf{l}_{\mathrm{n}}{}^{\mathrm{T}})\mathbf{J}_{\mathrm{ai},\widetilde{\Theta}} \tag{B.2d}$$

6. References

[1] J.P. Merlet, Parallel robots, Kluwer Academic Publisher, Netherlands, 2000.

[2] J. Gallardo, J.M. Rico, A. Frisoli, D. Checcacci, M. Bergamasco, Dynamic of parallel manipulators by means of screw theory, Mechanism and Machine Theory 38 (2003) 1113-1131

[3] A. Lopes, F. Almeida, A force-impedance controlled industrial robot using an active robotic auxiliary device, Robotics and Computer-Integrated Manufacturing 24 (2008) 299-309.

[4] Y.N. Wu, C. Gosselin, Design of reactionless 3-DOF and 6-DOF parallel manipulators using parallelepiped mechanisms, IEEE Transactions on Robotics 21 (5) (2005) 821-833

[5] D. Stewart, A platform with six degree of freedom: A new form of mechanical linage which enables a platform to move simultaneously in six degree of freedom developed by Elliot-Automation, Aircraft Engineering and Aerospace Technology 38 (4) (1965) 30-35.

[6] J.P. Merlet, Parallel manipulators: state of the art and perspectives, Advanced Robotics 8 (6) (1994) 589-596.

[7] K.H. Hunt, Structural kinematics of in-parallel-actuated robot-arms, ASME Journal of Mechanisms, Transmissions and Automation in Design 105(4) (1983) 705-712.

[8] W.Q.D. Do, D.C.H. Yang, Inverse dynamic analysis and simulation of a platform type of robot, Journal of Robotic Systems 5 (1988) 209-227.
[9] M. Honegger, R. Brega, G. Schweizer, Application of a nonlinear adaptive controller to a 6 dof parallel manipulator, In Proceeding of the 2000 IEEE International Conference on Robotics and Automation, San Francisco, CA, USA, (2000) pp. 1930-1935.
[10] D.H. Kim, J.Y. Kang, K-II. Lee, Robust tracking control design for a 6 DOF parallel manipulator, Journal of Robotics Systems 17(10) (2000) 527-547.
[11] C.C. Nguyen, S.S. Antrazi, Z.L. Zhou, C.E. Campbell, Adaptive control of a Stewart platform-based manipulator, Journal of Robotics Systems 10(5) (1992) 657-687.
[12] H.S. Kim, Y.M. Cho, K-II. Lee, Robust nonlinear task space control for a 6 DOF parallel manipulator, Automatica 41 (2005) 1591-1600.
[13] Y. Ting, Y.S. Chen, H.C. Jar, Modeling and control for a Gough-Stewart platform CNC machine, Journal of Robotics System 21(11) (2004) 609-623.
[14] J.L. Chen, W.D. Chang, Feedback linearization control of a two-link robot using a multi-crossover genetic algorithm, Expert Systems with Applications 36 (2009) 4154-4159.
[15] K.J. Astrom, T. Hagglund. PID Controllers: Theory, Design, and Tuning. Instrument Society of America: NC, 1995.
[16] Y.X Su, B.Y. Duan, C.H. Zheng, Y.F. Zhang, G.D. Chen, J.W. Mi, Disturbance-rejection high-precision motion control of a Stewart platform, IEEE Transactions on Control Systems Technology 12(3) (2004) 364-374.
[17] E. Burdet, M. Honegger, A. Codourey, Controllers with desired dynamic compensation and their implementation on a 6 DOF parallel manipulator, Proceeding of the 2000 IEEE/RSJ International Conference on Intelligent Robots and Systems, 2000, pp. 39-45.
[18] J.R. Noriega, H. Wang, A direct adaptive neural-network control for unknown nonlinear systems and its application, IEEE Transactions on Neural Networks 9 (1) (1998) 27-34.
[19] N.I. Kim, C.W. Lee, High speed tracking control of Stewart platform manipulator via enhanced sliding mode control, In Proceeding of the 1998 IEEE Conference on Robotics and Automation, Leuven, Belgium, (1998) pp. 2716-2721.
[20] I. Cervantes, J.A. Ramirez, On the PID tracking control of robot manipulators, Systems & Control Letters 42 (2001) 37-46.
[21] I. Davliskos, E. Papadopoulous, Model-based control of 6-DOF electrohydraulic parallel manipulator platform, Mechanism and Machine Theory 43 (2008) 1385-1400.
[22] F. Behi, Kinematic analysis for a six-degree-of-freedom 3-PRPS parallel mechanism, IEEE Journal of Robotics and Automation 4(5) (1988) 561-565.
[23] D.M. Ku, Direct displacement analysis of a Stewart platform mechanism. Mechanism and Machine Theory 34 (1999) 453-465.
[24] B. Dasgupta, T.S. Mruthyunjaya, A Newton-Euler formulation for the inverse dynamics of the Stewart platform manipulator, Mechanism and Machine Theory 33(8) (1998) 1135-1152.
[25] S.H. Koekebakker, Model based control of a flight simulator motion system. Ph.D Thesis. Netherlands: Delft University of Technology, 2001.
[26] H.E. Merrit, Hydraulic Control Systems, Wiley, 1967.
[27] D. Rowell, D.N. Wormley, System Dynamics: An Introduction, Prentice Hall, 1997.
[28] R. Gorez, Globally stable PID-like control of mechanical systems, Systems & Control Letters 38 (1999) 61-72.
[29] C.F. Yang, J.F. He, J.W. Han, X.C. Liu, Real-time state estimation for spatial six-degree-of-freedom linearly actuated parallel robots. Mechatronics 19(6) (2009) 1026-1033.

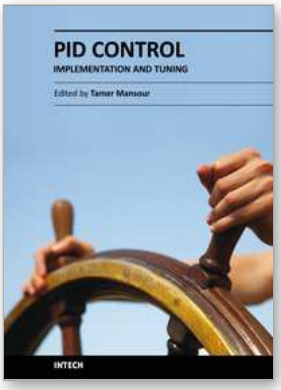

PID Control, Implementation and Tuning

Edited by Dr. Tamer Mansour

ISBN 978-953-307-166-4
Hard cover, 238 pages
Publisher InTech
Published online 19, April, 2011
Published in print edition April, 2011

The PID controller is considered the most widely used controller. It has numerous applications varying from industrial to home appliances. This book is an outcome of contributions and inspirations from many researchers in the field of PID control. The book consists of two parts; the first is related to the implementation of PID control in various applications whilst the second part concentrates on the tuning of PID control to get best performance. We hope that this book can be a valuable aid for new research in the field of PID control in addition to stimulating the research in the area of PID control toward better utilization in our life.

INTECH
open science | open minds

InTech Europe
University Campus STeP Ri
Slavka Krautzeka 83/A
51000 Rijeka, Croatia
Phone: +385 (51) 770 447
Fax: +385 (51) 686 166
www.intechopen.com

InTech China
Unit 405, Office Block, Hotel Equatorial Shanghai
No.65, Yan An Road (West), Shanghai, 200040, China
中国上海市延安西路65号上海国际贵都大饭店办公楼405单元
Phone: +86-21-62489820
Fax: +86-21-62489821